International Journal of Electrical and Computer Engineering (IJECE)
Vol. 16, No. 2, April 2026, pp. 638~650
ISSN: 2088-8708, DOI: 10.11591/ijece.v16i2.pp638-650

Dynamic analysis of a human-transporting robot climbing stairs

Duong Tan Dat, Le Hong Ky, Tran Duc Thuan
Department of Mechatronics, Faculty of Mechanical Engineering, Vinh Long University of Technology Education, Vinh Long, Vietnam

Article Info

Article history:

Received Aug 29, 2025
Revised Jan 3, 2026
Accepted Jan 16, 2026

Keywords:

Anti-roll mechanism
Balancing mechanism
Dynamic analysis
Human transport robot
Stair-climbing robots

ABSTRACT

Robots used for transporting people on stairs face several limitations regarding tipping and safety hazards. Changes in the robot's center of gravity during stair climbing can generate tipping moments, leading to instability, tipping, and increased danger to users. This paper presents the modeling and analysis results of a tracked robot for transporting people on stairs, equipped with an anti-tipping mechanism based on center of gravity balance, combined with a vibration-damping mechanism mounted at the rear of the robot to enhance stability during stair climbing. Based on Newton-Euler's formulas, robot dynamics equations are established to describe the motion and analyze the robot's stability characteristics. Simulation and experimental results investigating the changes in center of gravity, velocity, tipping moment, and balancing moment of the robot during uphill and downhill movement were performed using MATLAB Simulink software. Simulation results indicate that the robot's center of gravity is adjusted and stabilized throughout both uphill and downhill movements. Practical experiments conducted on a fabricated robot model, capable of carrying a 100 kg load and moving up and down stairs with a 35-degree incline, demonstrated the feasibility and effectiveness of the proposed mechanical design. The results showed good agreement in kinematic trends between experimental and simulated data during the stair climbing, stair-on, and stair-step transition phases. This agreement between experimental and simulation results proved the correctness of the robot system and the constructed dynamic model. The research results provide a basis for developing control algorithms for robots that efficiently transport people up and down stairs in buildings.

Corresponding Author:

Duong Tan Dat
Department of Mechatronics, Faculty of Mechanical Engineering, Vinh Long University of Technology Education
73 Nguyen Hue Road, Long Chau Ward, Vinh Long City, Vietnam
Email: datdt@vlute.edu.vn

1. INTRODUCTION

People with lower limb disabilities have difficulty moving up and down high-rise buildings without elevators. Robots capable of transporting people are devices that solve the current mobility difficulties for people with disabilities. However, limitations in tipping over, oscillating, and the inability to adapt to the height of stairs have reduced their reliability for users. Stair-climbing robots have been studied in many different forms, such as wheeled moving mechanisms [1], [2], tracked mechanisms [3], [4], claw-like mechanisms [5], [6], leg-like mechanisms [7], [8], and hybrid moving mechanisms [9], [10]. Although studies have shown the stair-climbing ability of robots, the ability to transport people to different terrains is still limited [11], [12]. Tao *et al.* [13] built a dynamic model for a tracked robot moving on stairs and showed the superior stair-climbing ability of this robot. However, the robot does not yet have a balancing and anti-roll mechanism, so the challenge of tipping over and oscillation during movement remains unresolved. The

problem of center of gravity deviation when the robot moves on steep terrain is the cause of the tendency to tip over during operation, especially when carrying loads on complex terrain such as stairs.

Several solutions for adjusting the center of gravity, such as using pneumatic mechanisms [14], auxiliary support mechanisms [15], X-shaped lifting mechanisms [16], and pendulum-type balancing mechanisms [17]–[19] have been proposed to address the problems of tip over, imbalance, oscillation reduction, and stability maintenance. However, these studies still face many challenges regarding robot size, stability, and adaptability to different staircases. Gao *et al.* [20] used classical mathematical methods to analyze the operation of a robot with a coiled tail rod mechanism to balance its center of gravity. However, the research was not feasible in the process of transporting people. The dynamics of a wheelchair moving with a wheel assembly and a support mechanism were studied [21]. The robot moving up stairs without a load showed the ability to climb stairs and stability at a fixed stair size. Research by Tian-ci Jiang and Grzegorz Dobrzyński analyzed the types of robots capable of climbing stairs and proposed a robot design with a user-controlled center of gravity to limit tipping; however, the results were only simulations [22], [23]. Robots capable of seat adjustment and damping are designed in 3D software proposed by Prof. S.M. Ramnani and colleagues; however, the current system is limited in size and the automatic capabilities of the balancing and anti-tilting system [24]. Dobrzyński *et al.* [25] uses a balancing slider to perform the process of moving up stairs; the robot's dynamic equations are also presented, but still in a 3D environment, and oscillations exist. Chawaphan *et al.* [26] using sensors in the process of center of gravity control is also somewhat feasible, although it is in the testing phase. Some robots can carry loads from 3 kg to 120 kg [27] and can move on stairs; however, the center of gravity control process is not yet capable of moving on different steps, and the structure is quite complex [28]. Based on the kinematic equations and dynamics of the robot, a closed-loop error control system to maintain stability during the robot's movement was studied [29], [30]. Current studies have achieved some success in the process of the robot moving up stairs; however, it is still not truly effective in transporting people up and down stairs.

In this study, a model of a robot transporting people upstairs using tracks, employing linear actuators in anti-roll control and oscillation reduction, is proposed. The change in the robot's center of gravity according to the stair slope is evaluated through the dynamic equations built throughout the operation. The results of the analysis and evaluation of the robot's operating state are verified in simulation and experiment to confirm the correctness of the constructed dynamic equations and to serve as a basis for building an anti-roll control algorithm for the robot transporting people.

2. HUMAN TRANSPORT ROBOT MODEL

2.1. Building a model of a human transport robot

The human transport robot is designed move on flat surfaces using wheels and to ascend stairs with crawlers. The balancing mechanism is connected to the seat, automatically adjusting the robot's center of gravity to change according to the slope of the stairs. The anti-roll mechanism behind performs the task of supporting the worker, reducing vibration, and increasing the robot's anti-roll ability. The robot is designed to always be in contact with at least two steps, which helps prevent falling by ensuring stable contact points. The schematic diagram Figure 1(a) and 3D model of the human transport robot are shown in Figure 1(b). The robot performs one-way movement up and down stairs, moves upstairs with a backward movement, and moves down stairs in the forward direction, in the same direction as the user's view.

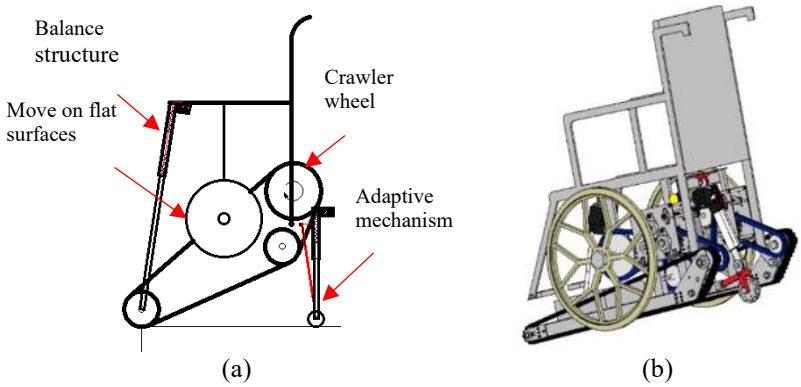

Figure 1. Human transport robot model (a) schematic diagram and (b) 3D model

2.2. Dynamics of a robot transporting people up and down stairs

The dynamic equations of robot transporting people are considered with movement on a flat surface using circular wheels, as shown in Figure 2(a), and movement on stairs using tracks as Figure 2(b). The robot's coordinate system is established at the position of the passive track at the front of the robot, with the OX axis parallel to the ground and the OY axis perpendicular to it. The robot's center of gravity G_{CR} begins to change when the robot switches to stair movement mode. The robot's center of gravity is determined by the relationship between the center of gravity of the robot frame $G_R(l_{Rx},\ l_{Ry})$ and the center of gravity of the seat $G_n(l_{nx},\ l_{ny})$. The center of gravity of the seat is adjusted according to the change in the robot's tilt angle.

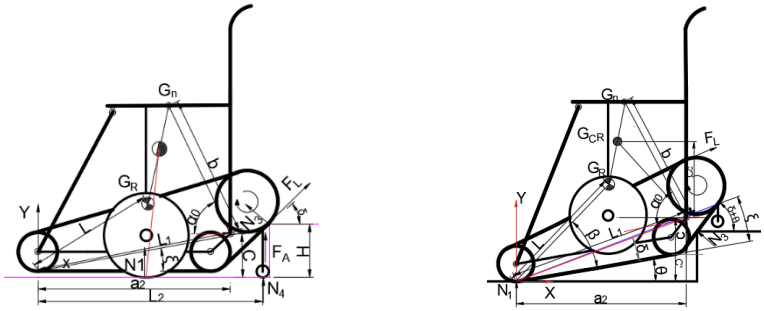

(a) (b)

Figure 2. The robot's stair-climbing phase in (a) while on a flat surface and (b) climbing the first step

The center of gravity of the robot frame and the center of gravity of the seat when the robot moves on a plane (Figure 2(a)) are set as (1):

$$\begin{cases} l_{Rx} = L\cos\beta \\ l_{Ry} = L\sin\beta \end{cases}; \begin{cases} l_{nx} = a_2 - b\cos\alpha_0 \\ l_{ny} = C + b\sin\alpha_0 \end{cases} \quad (1)$$

Where $l_{Rx}(mm), l_{Ry}(mm)$ is the coordinate of the robot frame's center of gravity, and $l_{nx}(mm), l_{ny}(mm)$ is the coordinate of the seat along the OX and OY axes, L(mm) is the distance between the coordinate system and the center of gravity, L_1 (mm) is the distance between the passive wheel and the position of the chair's rotation axis along the x-axis, C (mm) is the distance from the chair's rotation axis to the ground, $\alpha_0(^0)$ is the chair's rotation angle, $\beta(^0)$ is the angle of the robot frame's center of gravity relative to the track surface, b (mm) is the distance from the chair's center of gravity to the rotation axis, $a_2(mm)$ is the projection of the distance from the coordinate axis to the angle of rotation onto the OX axis.

As it moves, the robot begins to tilt at an angle θ according to the slope of the stairs, as shown in Figure 2(b). The robot's coordinate system is set according to the tilt as (3):

$$\begin{cases} l_{Rx} = L\cos(\beta+\theta) \\ l_{Ry} = L\sin(\beta+\theta) \end{cases}; \begin{cases} l_{nx} = L_1\cos(\theta+\delta) - b\cos\alpha_0 \\ l_{ny} = C + L_1\sin(\theta+\delta) + b\sin\alpha_0 \end{cases} \quad (2)$$

The robot's center of gravity $G_{cR}(l_{cx}, l_{cy})$ is determined using the coordinates of the robot frame's center of gravity G_R and the seat's center of gravity G_n based on the tilt angle (θ). The position l_{cx}, l_{cy} is set as formula (3), and it is automatically adjusted according to the tilt angle. The robot center of gravity position is adjusted to be stable at the initial position, which can limit the phenomenon of tipping over, and the seat center of gravity determines the robot center of gravity position.

$$\begin{cases} l_{cx} = \frac{m_n l_{nx} + m_R l_{Rx}}{m_e} \\ l_{cy} = \frac{m_n l_{ny} + m_R l_{Ry}}{m_e} \end{cases} \Rightarrow \begin{cases} \dot{l}_{cx} = \frac{m_n \dot{l}_{nx} + m_R \dot{l}_{Rx}}{m_e} \\ \dot{l}_{cy} = \frac{m_n \dot{l}_{ny} + m_R \dot{l}_{Ry}}{m_e} \end{cases} \quad (3)$$

Where $m_n(kg)$, $m_R\ (kg)$ is the mass of the person and the mass of the robot; $m_e(kg) = m_R + m_n$ is the total mass of the robot. The operating state of the robot when climbing stairs is shown in Figure 3.

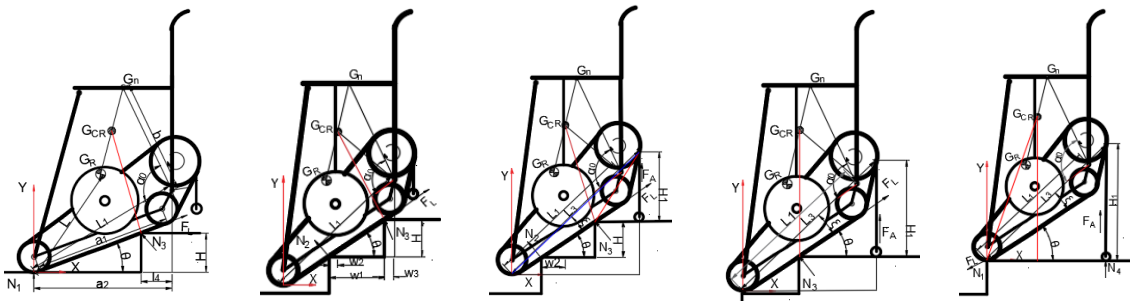

(a) (b) (c) (d) (e)

Figure 3. Stages of the robot climbing stairs: (a) first step, (b) ascending, (c) preparing to mount the landing, (d) final step, and (e) descending

The robot moves on a flat surface using circular wheels, with the assistance of auxiliary support wheels to help it adapt to the stairs, as shown in Figure 2(a). During this phase, the robot prepares to climb the stairs, and the circular wheels are assumed to reach the maximum Coulomb friction limit. The kinematic equations are established as (4):

$$\begin{aligned}
&\sum F_x = F_L\cos\delta - N_3\, sin\,\delta + \frac{\eta m_e g l_p}{l_p + l_w + \eta l_{cy}} = \mathrm{m}_e \ddot{l}_{cx} \\
&\sum F_y = -\, m_e g + N_1 + N_4 + N_3(cos\,\delta + \eta\, sin\,\delta) = 0 \\
&\sum M_R = N_1 l_w - N_4 l_p - \frac{\eta m_e g l_p}{l_p + l_w - \eta l_{cy}} l_{cy} = 0 \\
&l_p = L_2 - l_{cx}
\end{aligned} \tag{4}$$

Where $N_1(N)$, $N_4\,(N)$, $N_3(N)$ is the reaction force, l_p (mm) is the distance between the robot's center of gravity and the support wheel position; l_w (mm) is the distance between the robot's wheel on the ground; η is the coefficient of friction; F_L (N) is the traction force of the crawler; δ (^{0}) is the crawler angle, $g\ (m/s^2)$ is the acceleration of gravity, $L_2(mm)$ is the distance from the coordinate system to the auxiliary support wheel.

The dynamic equations describing robot motion during the ascent of the first stair step, as illustrated in Figure 3(a), are formulated as (5):

$$\begin{aligned}
&\sum F_x = F_L\, cos(\,\theta) + \eta N_1\, cos(\,\theta) - N_3\, sin(\,\theta) = m_e \ddot{l}_{cx} \\
&\sum F_y = F_L \sin(\theta) + N_1 + N_3 \cos(\theta) - m_e g = m_e \ddot{l}_{cy} \\
&\sum M_R = m_e g(a_2 - l_{cx} - l_4) + N_1(\eta H - L_1 \cos\theta - l_4) = [I_s + m_e R_{c1}^2]\ddot{\theta} \\
&R_{c1} = \sqrt{(a_2 - l_{cx} - l_4)^2 + (l_{cy} - H)^2}
\end{aligned} \tag{5}$$

Where R_{c1} (mm) is the distance from the robot's center of gravity to the first step, l_4 (mm) is the distance from the step to the center of the chair's pivot axis, H (mm) is the step height, and $I_s(kg.m^2)$ is the moment of inertia.

The robot's overturning moment is largest when the crawler moves completely on the step and only contacts two steps, see Figure 3(b). The dynamic equation of the robot in contact with two steps is presented as (6):

$$\begin{aligned}
&\sum F_x = F_L \cos(\theta) + \eta(N_2 - N_3)\cos(\theta) \text{- } \mathrm{N}_2\, sin(\,\theta) = m_e \ddot{l}_{\mathrm{cx}} \\
&\sum F_y = F_L\, sin(\,\theta) + \eta(N_2 + N_3)\, sin(\,\theta) + (N_2 + N_3)\, cos(\,\theta) - m_e g = m_e \ddot{l}_{cy} \\
&\textstyle\sum M_R = F_L(w_1 \sin(\theta) \text{ - } \mathrm{H}\cos(\theta)) \text{ - } m_e \mathrm{g} w_2 + N_3(\eta H + w_1) = 0
\end{aligned} \tag{6}$$

Where w_2 (mm) is the distance from the first step to the projection of the center of gravity in the direction of movement, w_1 (mm) is the width of the step.

The robot experiences an imbalance and flips backward as it begins to leave the staircase, as shown in Figure 3(c). The greater the distance from the robot's center to the last step of the staircase R_{c3} (mm), the further the robot's center of gravity shifts backward. The thrust force $F_A(N)$ d from the electric cylinder of the damping mechanism prevents the robot from flipping backward. The dynamic equation for damping the robot is as (7):

$$\sum F_x = F_L\cos\theta - \eta(N_3 + \mathrm{N}_4 - N_2)\cos\theta + F_A\cos(\theta+\xi) - (N_3 + \mathrm{N}_2)\sin\theta = m_e(\ddot{l}_{\mathrm{cx}}\cos\theta + \ddot{l}_{\mathrm{cy}}\sin\theta)$$
$$\sum F_y = F_L\sin\theta + \eta(N_2+N_3)\sin\theta + (N_2+N_3)\cos\theta + N_4 + F_A\sin(\theta+\xi) - m_e g\cos\theta = m_e[\ddot{l}_{cx}\sin\theta + \ddot{l}_{cy}\cos\theta]$$
$$\sum M_R = F_L(\mathrm{H}\cos\theta - w\sin\theta) + F_A\frac{\Delta L}{\tan\theta} + N_2(H\sin\theta + w\cos\theta) + N_4\frac{\Delta L}{\tan\theta} - m_e g(L_3\cos(\theta+\xi) - \frac{\Delta L}{\tan\theta} - l_{\mathrm{cx}}) = (I_s + m_e R_{c3})\ddot{\theta}$$
$$R_{c3} = \sqrt{(L_3\cos(\theta+\xi) - \tfrac{\Delta L}{\tan\theta} - l_{\mathrm{cx}})^2 + \left(l_{cy} - (L_3\sin(\xi+\theta) - H_1)\right)^2} \quad (7)$$

Where $H_1(mm)$ l is the cylinder length, $\Delta L(mm)$ is the displacement of the electric cylinder, $L_3(mm)$ is the distance of the vibration-damping mechanism from the coordinate system, and $\xi(^0)$ is the angle of the vibration-damping mechanism relative to the track surface.

The robot reaches the final step with the auxiliary support structure engaged, as shown in Figure 3(d). Although the robot's center of gravity is located on the stair platform, a backward tipping tendency still exists. Accordingly, the dynamic equations for this stage are given by (8).

$$\sum F_x = F_L\cos\theta + \mathrm{F}_A\cos(\theta+\xi) - \eta(N_3+N_4)\cos\theta - N_3\sin\theta = m_e(\ddot{l}_{cx}\cos\theta + \ddot{l}_{cy}\sin\theta)$$
$$\sum F_y = F_L\sin\theta + \mathrm{F}_A\sin(\theta+\xi) + \eta(N_3-N_4)\sin\theta + N_3\cos\theta + N_4 - m_e\mathrm{g}\cos\theta = m_e(\ddot{l}_{cy}\cos\theta - \ddot{l}_{cx}\sin\theta)$$
$$\sum M_R = F_L\frac{\Delta L}{\tan\theta}\sin\theta + N_3 w_2\sin\theta + F_A\frac{\Delta L}{\tan\theta} - m_e g(l_{cx} - L_3\cos(\theta+\xi) - \tan\theta\,(L_3\sin(\theta+\xi) - H_1) = (I_s + m_e R_{c4})\ddot{\theta}$$
$$R_{c4} = \sqrt{(lcx - (L_3\cos(\theta+\xi) - \tan\theta\,(L_3\sin(\theta+\xi) - H_1))^2 + \left(l_{cy} - (L_3\sin(\theta+\xi) - H_1)\right)^2} \quad (8)$$

Where R_{c4} (mm) is the distance from the center of gravity to the last step of the staircase.

At the end of the uphill phase, the robot's tilt angle returns to its original position. Next, the robot begins the downhill phase as shown in Figure 3(e). The robot adapts to the stair slope using an auxiliary support mechanism. The anti-roll mechanism adjusts the robot's center of gravity linearly according to the change in tilt angle. The dynamic equations for the robot's downhill movement are presented as (9):

$$\sum F_x = F_L\cos\theta + F_A\cos(\theta+\xi) - \eta(N_1+N_4)\cos\theta = m_e[\ddot{l}_{\mathrm{cx}}\cos\theta + \ddot{l}_{\mathrm{cy}}\sin\theta]$$
$$\sum F_y = F_L\sin\theta + N_1 + N4 + F_A\sin(\theta+\xi) - \eta(N_1+N_4)\sin\theta - m_e g = m_e[\ddot{l}_{\mathrm{cy}}\cos\theta - \ddot{l}_{\mathrm{cx}}\sin\theta]$$
$$\sum M_R = F_A L_3\cos(\theta+\xi) + F_L L_4 - \eta N_4(H_1\tan(\xi+\theta) - l_{cx}) - m_e g l_{cx}\sin\theta = (I_s + m_e R_{c6})\ddot{\theta}$$
$$R_{c6} = \sqrt{l_{cx}^2 + l_{cy}^2} \quad (9)$$

3. SIMULATION AND EXPERIMENTATION

3.1. Simulation results

The simulation was set up in MATLAB Simulink software and used the equations developed in section 2 to evaluate the variation of the center of gravity, oscillation phenomena, and the system's ability to adapt to changes in the tilt angle. The input signal is a step function signal; the parameters used in the simulation are presented in Table 1. Simultaneously, assumptions about slippage, non-linear robot movement, and instantaneous effects when the robot goes up and down stairs were ignored.

Table 1. The parameters used for simulation

Symbol	Description	Value	Unit
ω	Maximum motor speed (assumed)	2000	RPM
m_e	Robot mass	150	Kg
L_1	Distance from the seat rotation axis to the driven wheel	800	mm
a_2	Distance of the seat pivot axis projection onto the ox axis	500	mm
L_3	Distance from the auxiliary support mechanism to the driven wheel	900	mm
F_L	Traction force	1720	N
F_A	Electric actuator lifting force	1000	N
I_s	Moment of inertia	120	$kg.m^2$
g	Gravitational acceleration	9.8	m/s^2
η	Coefficient of friction	0.6	
ΔL	Auxiliary support mechanism stroke (assumed)	300	mm
θ	Tilt angle	35	°
ξ	Angle between the auxiliary support mechanism and the X-axis	30	°
H	Stair height	150	mm
w_1	Stair width	300	mm

The simulation results of the robot's center of gravity and dynamic moment over time are presented in Figure 4. The results show that the velocity at the robot's center of gravity along the X-axis reaches a maximum in about 0.25 seconds, then gradually decreases in Figure 4(a). Initially, the forward velocity along the X-axis increases until the robot reaches the first step, then tends to decrease. The velocity along the Y-axis decreases rapidly and reaches a minimum in about 0.2 seconds, then begins to increase slightly with the angle of inclination θ in Figure 4(b). Regarding the position of the center of gravity along the X-axis, it increases, then decreases towards the slope of the stairs in Figure 4(c), while the position along the Y-axis initially decreases slightly, then stabilizes and begins to increase at 0.5 seconds in Figure 4(d). The results of the moment survey of the robot's center of gravity show that the robot is in a fairly stable state, without tipping over. The balancing moment of the robot's center of gravity increases rapidly and stabilizes in 0.5 seconds, as shown in Figure 4(e). The robot's overturning moment reaches a maximum in the first 0.7 seconds and then gradually decreases in Figure 4(f). The tilt angle θ varies over time, as shown in Figure 4(g), describing the variation of the robot's inclination while ascending the stairs.

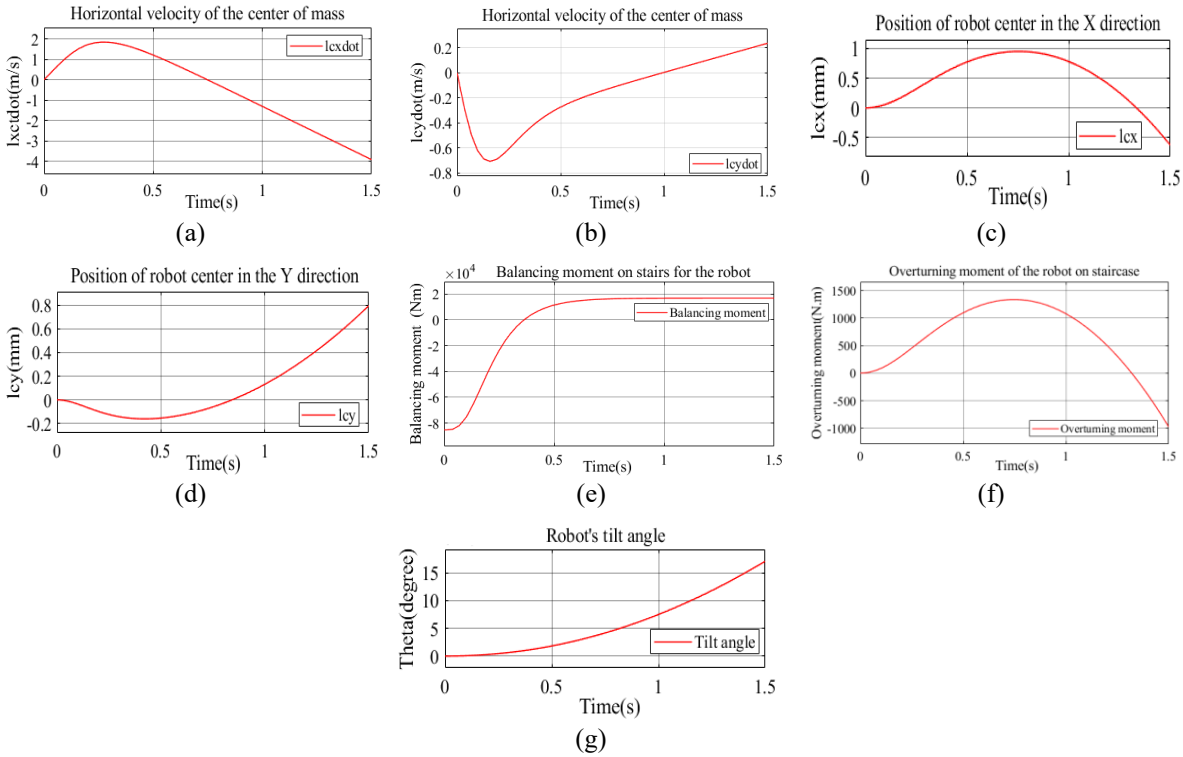

Figure 4. Simulation results of the initial stair-climbing stage: (a)–(d) center-of-gravity velocities and positions along the X- and Y-axes, (e) balancing moment, (f) overturning moment, and (g) inclination angle

Figure 5 presents the simulation results of the phase while on the stairs, showing that the robot's center of gravity velocity reaches its maximum in 0.25 seconds and then gradually decreases, as shown in Figure 5(a), and the velocity along the oy axis reaches its minimum and increases after 0.2 seconds in Figure 5(b). During the phase when the robot is moving up the stairs, the center of gravity along the x-axis tends to reach its maximum and then gradually decrease in Figure 5(c), while the center of gravity along the Y-axis gradually decreases over time in Figure 5(d), indicating that the center of gravity balancing mechanism is working and gradually stabilizing. The balancing moment increases rapidly and reaches a steady value as the robot fully ascends the staircase in Figure 5(e). The overturning moment remains nearly constant in Figure 5(f), indicating stable robot behavior during stair climbing.

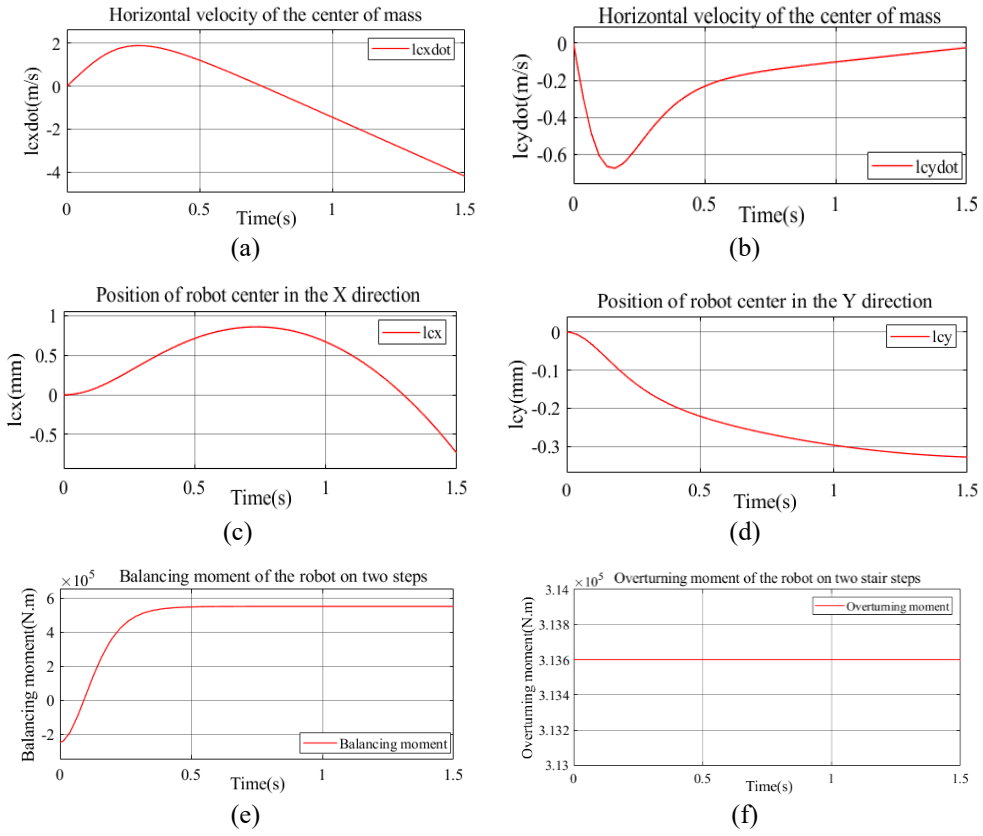

Figure 5. Simulation results for the robot operating on two stair steps: (a)–(d) center-of-gravity velocities and positions along the X- and Y-axes, (e) balancing moment of the center of gravity, and (f) overturning moment of the center of gravity

The simulation results show that the X-axis and Y-axis as shown in Figures 6(a) and 6(b) velocity of the robot's center of gravity at the last step of the staircase fluctuates in the first 0.15 seconds, after which the velocity gradually increases. This indicates that the robot is switching the landing mode of the auxiliary support wheel and the effectiveness of the auxiliary support mechanism in preventing the robot from tipping over. The position of the center of gravity coordinates is stable in the first 0.4 seconds, then begins to increase gradually over time, as illustrated in Figures 6(c) and 6(d).

The simulation results show that the velocity during the preparation phase of descending the stairs is presented in Figure 7(a) and the position of its center of gravity is depicted in Figure 7(b) along the X-axis increase and then decreases gradually with the angle of inclination. The velocity along the Y-axis increases to a maximum in 0.4 seconds, then gradually decreases during the robot's ascent and descent towards the stair step as demonstrated in Figure 7(c). The center of gravity stabilizes and begins to increase gradually from 0.1 seconds during operation as shown in Figure 7(d). The balancing moment slightly increases and then rapidly decreases within 0.5 seconds, after which it stabilizes, as shown in Figure 7(e). When the robot descends the stairs, an overturning moment initially appears. However, it rapidly decreases after 0.3 seconds, as shown in Figure 7(f), indicating that the system achieves balance and the robot operates in an adaptive state.

The balancing mechanism adjusts the center of gravity to prevent the robot from tipping over in operating scenarios, as shown in Figure 8. The electric cylinder stroke needs to be adjusted to prevent tipping when the seated person falls forward as illustrated in Figure 8(a), when the robot moves fully up the slope of the stairs as illustrated in Figure 8(b), when the robot reaches the last step of the stairs as illustrated in Figure 8(c), and when moving down the stairs as illustrated in Figure 8(d).

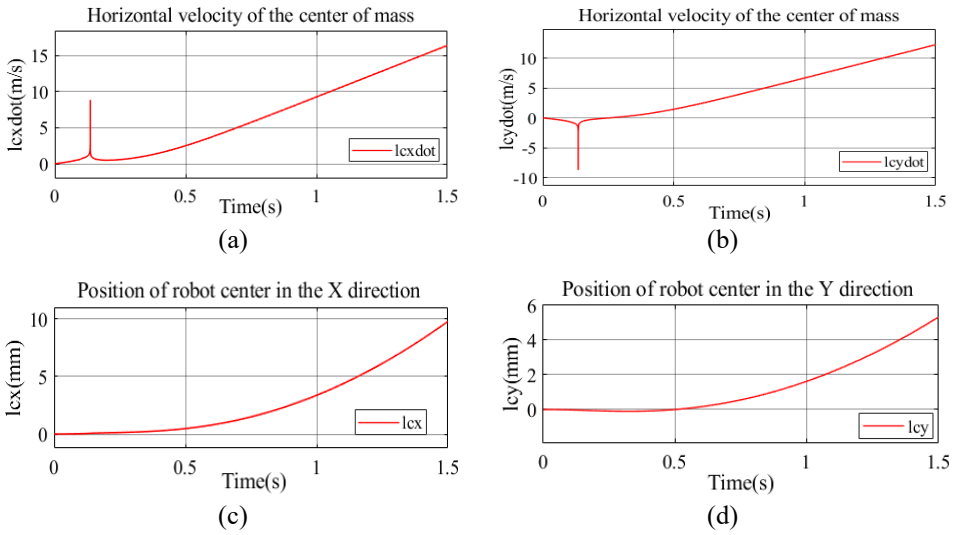

Figure 6. Simulation results of the robot's center of gravity at the last step of the staircase: (a)–(d) center-of-gravity velocities and positions along the X- and Y-axes

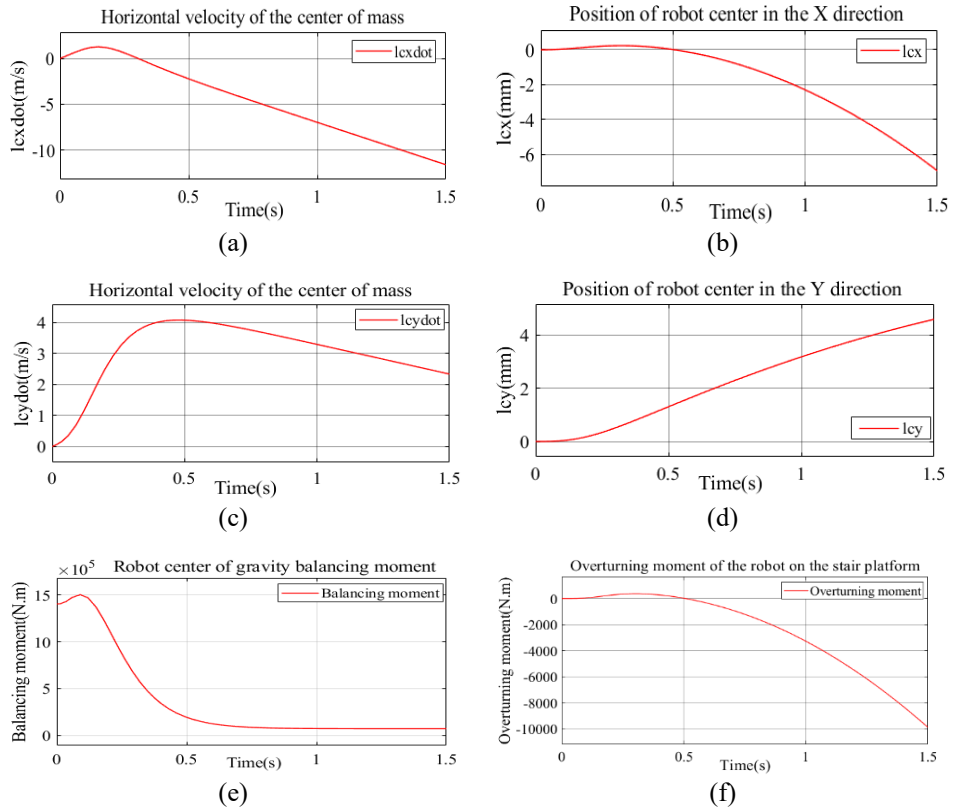

Figure 7. Simulation results for the robot preparing to descend the staircase: (a)–(d) center-of-gravity velocities and positions along the X- and Y-axes, (e) balancing moment on the stair platform, and (f) overturning moment

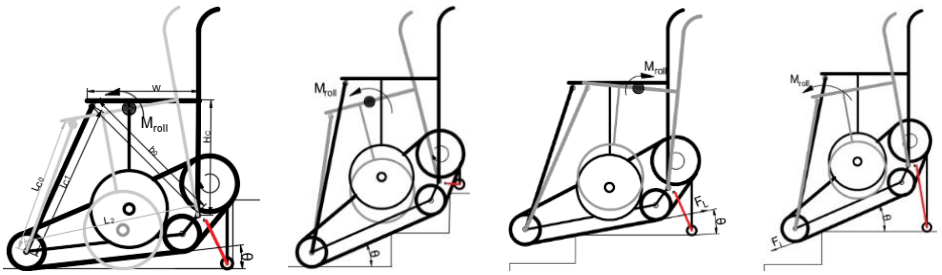

Figure 8. Overturning-prone states of the human transport robot during stair negotiation: (a) first-step climbing, (b) fully moving up the stairs, (c) transferring to the support platform, and (d) stair descent

Suppose the seat is designed with a width $w(mm)$, a seat height $H_c(mm)$, $b_0(mm)$ is the position where the cylinder is placed on the seat, $l_{c0}(mm), l_{c1}(mm)$ is the initial stroke and operating stroke of the electric cylinder, $l_5(mm)$ is the distance from the cylinder to the seat rotation axis. The displacement distance $\Delta l_{xl}(mm)$ that can stabilize the center of gravity when the robot moves up the slope θ is designed as:

$$\Delta l_{xl} = L_{c1} - l_{c0} = \sqrt{l_5^2 + b_0^2 - 2l_5 b_0 \, cos(\delta - \theta)} - l_{c0}$$

From the simulation results of the robot's center of gravity, the required cylinder stroke in the balancing mechanism was determined to ensure anti-tipping operation. The simulation results of the cylinder stroke are presented in Figure 9, showing that a required cylinder stroke of 300 mm can ensure stable robot movement on a 35-degree staircase.

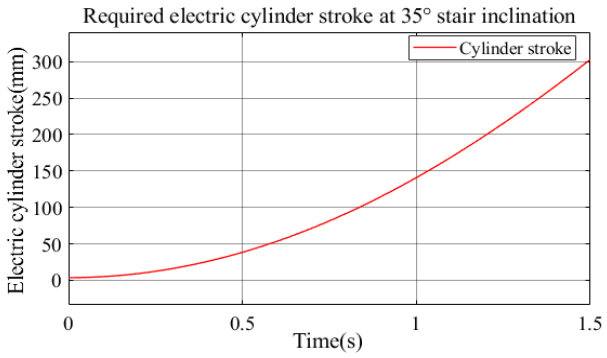

Figure 9. Balancing actuator stroke estimated from center-of-gravity simulation results

3.2. Experiment results

Experimental results were obtained using a fabricated human transport robot model. The robot moved up a 35-degree slope staircase with a 300 mm wide and 150 mm high step as illustrated in the sequence in Figure 10, depicting the start of ascent, full positioning on the stairs, reaching the top, and the final step as shown in Figures 10(a) to 10(d). The robot carried a different weight at a speed of 0.5 m/s when ascending and 0.2 m/s when descending. Additionally, an electric cylinder with a movement speed of 0.03 m/s and a stroke of 300 mm was used to control the robot's center of gravity and auxiliary support mechanism. Control was performed via a remote-control system. The system used an IMU (6 DOF) sensor mounted on the robot's body to measure the tilt angle, and a rotary encoder mounted on the seat's pivot and track axles to determine the robot's center of gravity movement trend through the seat's center of gravity movement.

The experimental results were displayed on a computer via a wireless system. A real-time graph from the MATLAB Simulink software shows the results of the survey on the chair's movement velocity and the torque of the track axle as the robot moves up the stairs, as presented in Figure 11. The robot can move up and down the stairs safely without tipping over. In the initial phase, the torque on the left and right axles

increased rapidly for about 2 seconds and reached a maximum of 380 N·m, as shown in Figure 11(a). During the uphill phase, the torque remains almost constant, stabilizing at its maximum value for ascending the slope. During the ascending phase, the torque begins to decrease rapidly to zero. The chair's velocity increases rapidly in the first 10 seconds to balance the robot's body inclination. From the 10th to the 17th second, the velocity fluctuates slightly and decreases as the robot begins to move towards the last step of the stairs. From the 17th second onwards, the robot ascends the stair platform and lowers its center of gravity, so the velocity increases slightly and gradually decreases to zero on the flat surface as illustrated in Figure 11(b). The chair's velocity fluctuates only slightly, indicating the robot's stability and safety during the stair climbing process.

Experiments have shown that the designed human-carrying robot can move up and down stairs. Simulation and experimental results show that the measured quantities tend to vary similarly over time. The comparison results are presented in Table 2.

The comparison results show that the dynamic trend of the system in simulation and in reality, is consistent, which demonstrates the correctness of the equations developed. However, the system is still limited in some stages, so on this basis, algorithms such as Fuzzy-PID [31], PD-SMC [32], and adaptive sliding [33] can be developed for control during the manufacturing and improvement of the human transport robot.

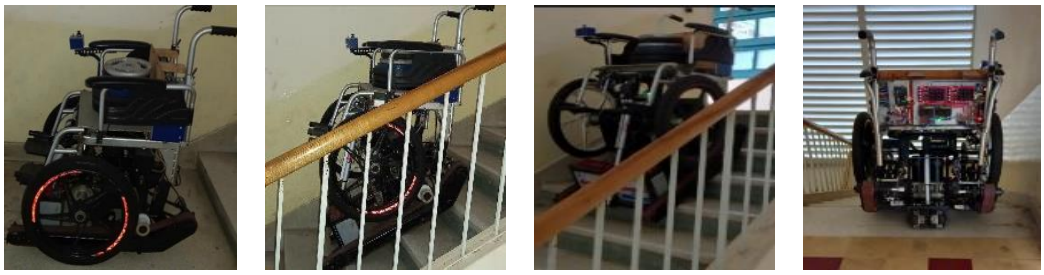

(a) (b) (c) (d)

Figure 10. Experimental results of the robot climbing a 35° staircase (a) start of stair ascent, (b) fully on the staircase, (c) reaching the end of the staircase, and (d) final stair step

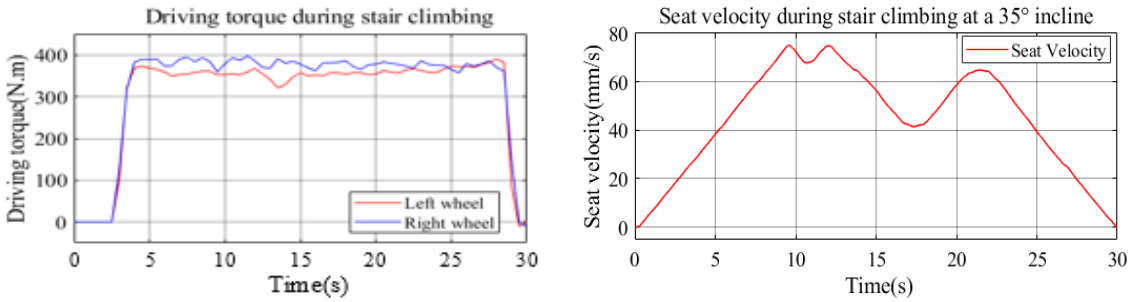

(a) (b)

Figure 11. Experimental results of robot moving up stairs (a) track axis torque and (b) chair velocity

Table 2. Comparison of simulation and experimental results

Phase	Simulation results		Experimental results		Remarks
	Center of mass velocity (m/s)	Tipping moment (N.m)	Seat velocity (m/s)	Drive torque (N.m)	
First-step climbing phase	Rapid increase → decrease	Increase → rapid decrease	Rapid increase	Rapid increase	Step-climbing state
Fully on the staircase	Slight increase → rapid decrease	Constant	Rapid increase	Steady state	Stable motion on the staircase
Final step-climbing phase	Oscillation → increase	Oscillation → rapid stabilization	Oscillation → slight increase → decrease	Constant	Transition to the landing platform
On the landing platform	Slight increase → rapid decrease	Slight increase → rapid decrease	Increase → gradual decrease to zero	Rapid decrease to zero	Effective balancing and vibration attenuation

4. CONCLUSION

This study developed a dynamic model of a robot for transporting people up and down stairs, capable of moving across various terrains with the participation of a balancing mechanism and an anti-tipping mechanism at the bottom of the stairs. Based on Newton-Euler's formulas, force and moment equations were established to check the velocity, position, and moment of the robot's center of gravity at different stages of movement. Simulation results showed that the velocity and center of gravity change proportionally with the slope, and the balancing moment and tipping moment remain stable during the up and down stair climbing phases. Based on the simulation, the robot's fabrication process and experiments showed that the robot can move up and down stairs stably without tipping over on a 35-degree slope, with a load capacity of 100 kg. Although the experiments only measured the chair velocity and axis torque, the experimental results are consistent with the simulation regarding the kinematic trend of the robot's changing velocity. Based on the equations developed and the results obtained, control algorithms such as adaptive control algorithms, optimization algorithms, and stability algorithms will be used in future robot control to help robots operate flexibly and stably in all terrains and carry different loads.

ACKNOWLEDGMENTS

The research team sincerely thanks the leaders of Vinh Long University of Technology Education and all lecturers of the Faculty of Mechanical Engineering for supporting and creating conditions for the research team to complete this research objective.

FUNDING INFORMATION

Authors state no funding involved.

AUTHOR CONTRIBUTIONS STATEMENT

This journal uses the Contributor Roles Taxonomy (CRediT) to recognize individual author contributions, reduce authorship disputes, and facilitate collaboration.

Name of Author	C	M	So	Va	Fo	I	R	D	O	E	Vi	Su	P	Fu
Duong Tan Dat	✓	✓	✓	✓	✓	✓	✓	✓	✓	✓	✓	✓	✓	✓
Le Hong Ky	✓			✓	✓	✓		✓	✓	✓	✓	✓	✓	✓
Tran Duc Thuan		✓		✓	✓				✓			✓	✓	

C : **C**onceptualization
M : **M**ethodology
So : **So**ftware
Va : **Va**lidation
Fo : **Fo**rmal analysis
I : **I**nvestigation
R : **R**esources
D : **D**ata Curation
O : Writing - **O**riginal Draft
E : Writing - Review & **E**diting
Vi : **Vi**sualization
Su : **Su**pervision
P : **P**roject administration
Fu : **Fu**nding acquisition

CONFLICT OF INTEREST STATEMENT

Authors state no conflict of interest.

INFORMED CONSENT

Informed consent was not applicable, as no human participants were involved in this study.

ETHICAL APPROVAL

This research did not involve the participation of human subjects or animals. Experimental validation was performed exclusively using mechanical loads representing human body weight on the robotic platform. In accordance with applicable regulations and publisher requirements, ethical approval was not required.

DATA AVAILABILITY

The data that support the findings of this study are available from the corresponding author, DTD, upon reasonable request.

REFERENCES

[1] Y. Onozuka, N. Tomokuni, G. Murata, and M. Shino, "Dynamic stability control of inverted-pendulum-type robotic wheelchair for going up and down stairs," in *IEEE International Conference on Intelligent Robots and Systems*, 2020, pp. 4114–4119, doi: 10.1109/IROS45743.2020.9341242.

[2] Y. Li *et al.*, "Kinematic modeling of a combined system of multiple Mecanum-Wheeled robots with velocity compensation," *Sensors (Switzerland)*, vol. 20, no. 1, Dec. 2020, doi: 10.3390/s20010075.

[3] A. Pappalettera, G. Reina, and G. Mantriota, "Design and analysis of tracked stair-climbing robot using innovative suspension system," *Robotics*, vol. 13, no. 3, pp. 1–18, 2024, doi: 10.3390/robotics13030045.

[4] P. Chatterjee, N. Lahiri, A. Bhattacharjee, and A. Chakraborty, "Automated hybrid stair climber for physically challenged people," in *2021 5th International Conference on Electronics, Materials Engineering and Nano-Technology, IEMENTech 2021*, Sep. 2021, pp. 1–4, doi: 10.1109/IEMENTech53263.2021.9614713.

[5] S. R. Thamel, R. Munasinghe, and T. Lalitharatne, "Motion planning of novel stair-climbing wheelchair for elderly and disabled people," in *MERCon 2020 - 6th International Multidisciplinary Moratuwa Engineering Research Conference, Proceedings*, 2020, pp. 590–595, doi: 10.1109/MERCon50084.2020.9185273.

[6] S. Nakajima and S. Sawada, "Methodology of climbing and descending stairs for four-wheeled vehicles," in *2020 IEEE 23rd International Conference on Intelligent Transportation Systems, ITSC 2020*, Sep. 2020, pp. 1–6, doi: 10.1109/ITSC45102.2020.9294695.

[7] S. Qi, W. Lin, Z. Hong, H. Chen, and W. Zhang, "Perceptive autonomous stair climbing for quadrupedal robots," in *IEEE International Conference on Intelligent Robots and Systems*, 2021, pp. 2313–2320, doi: 10.1109/IROS51168.2021.9636302.

[8] J. Ren, Z. Gu, H. Choset, and S. Yang, "Trajectory optimization for the legged system trajectory optimization for legged systems." 2020, doi: 10.13140/RG.2.2.36522.64963.

[9] J. Lee, W. Jeong, J. Han, T. Kim, and S. Oh, "Barrier-free wheelchair with a mechanical transmission," *Applied Sciences (Switzerland)*, vol. 11, no. 11, 2021, doi: 10.3390/app11115280.

[10] M. Klöppel *et al.*, "Scube-concept and implementation of a self-balancing, autonomous mobility device for personal transport," *World Electric Vehicle Journal*, vol. 9, no. 4, 2018, doi: 10.3390/wevj9040048.

[11] T. Seo, S. Ryu, J. H. Won, Y. Kim, and H. S. Kim, "Stair-climbing robots: A review on mechanism, sensing, and performance evaluation," *IEEE Access*, vol. 11, pp. 60539–60561, 2023, doi: 10.1109/ACCESS.2023.3286871.

[12] W. Tao, J. Xu, and T. Liu, "Electric-powered wheelchair with stair-climbing ability," *International Journal of Advanced Robotic Systems*, vol. 14, no. 4, pp. 1–13, 2017, doi: 10.1177/1729881417721436.

[13] W. Tao, Y. Ou, and H. Feng, "Research on dynamics and stability in the stairs-climbing of a tracked mobile robot," *International Journal of Advanced Robotic Systems*, vol. 9, 2012, doi: 10.5772/52850.

[14] H. Wang *et al.*, "The personal mobility and manipulation appliance (PerMMA): A robotic wheelchair with advanced mobility and manipulation," in *Proceedings of the Annual International Conference of the IEEE Engineering in Medicine and Biology Society, EMBS*, 2012, pp. 3324–3327, doi: 10.1109/EMBC.2012.6346676.

[15] J. Anjeneyulu and A. Purushotham, "Design and analysis of a stair climbing wheel chair," *International Journal of Scientific Research in Science, Engineering and Technology*, vol. 06, no. 1, pp. 430–435, 2019, doi: 10.32628/ijsrset196176.

[16] M. Zhang, J. Huang, and C. Jiang, "Research on multifunctional integrated intelligent stair-climbing chair based on ergonomics," in *E3S Web of Conferences*, 2021, vol. 260, doi: 10.1051/e3sconf/202126003011.

[17] B. Panomruttanarug and P. Chotikunnan, "Self-balancing iBOT-like wheelchair based on type-1 and interval type-2 fuzzy control," *2014 11th International conference on electrical engineering/electronics, computer, telecommunications and information technology (ECTI-CON)*, 2014, doi: 10.1109/ECTICon.2014.6839710.

[18] G. Quaglia and M. Nisi, "Design of a self-leveling cam mechanism for a stair climbing wheelchair," *Mechanism and Machine Theory*, vol. 112, pp. 84–104, 2017, doi: 10.1016/j.mechmachtheory.2017.02.003.

[19] B. D. Castillo, Y. F. Kuo, and J. J. Chou, "Novel design of a wheelchair with stair climbing capabilities," in *ICIIBMS 2015 - International Conference on Intelligent Informatics and Biomedical Sciences*, Nov. 2016, pp. 208–215, doi: 10.1109/ICIIBMS.2015.7439508.

[20] X. Gao, D. Cui, W. Guo, Y. Mu, and B. Li, "Dynamics and stability analysis on stairs climbing of wheel-track mobile robot," *International Journal of Advanced Robotic Systems*, vol. 14, no. 4, pp. 1–13, May 2017, doi: 10.1177/1729881417720783.

[21] P. Chawaphan, D. Maneetham, and P. N. Crisnapati, "Designing stair climbing wheelchairs with surface prediction using theoretical analysis and machine learning," *Indonesian Journal of Electrical Engineering and Computer Science*, vol. 38, no. 1, pp. 120–132, Apr. 2025, doi: 10.11591/ijeecs.v38.i1.pp120-132.

[22] T. C. Jiang, S. H. Yin, and E. Tanaka, "Wheelchair able to assist the elderly to move on stairs and stand up," in *2019 58th Annual Conference of the Society of Instrument and Control Engineers of Japan, SICE 2019*, 2019, pp. 1168–1173, doi: 10.23919/SICE.2019.8859944.

[23] G. Dobrzyński, "Classification of innovative wheelchair constructions with the option of transport via stairs," *WUT Journal of Transportation Engineering*, vol. 133, pp. 59–75, 2021, doi: 10.5604/01.3001.0015.6740.

[24] S. M. Ramnani, A. Pawar, S. Anawkar, S. Hire, and V. Giram, "Design and manufacturing of stair climbing wheelchair," *International Research Journal of Engineering and Technology*, vol. 7, no. 5, pp. 2003–2006, May 2020.

[25] G. Dobrzyński, W. Choromański, and I. Grabarek, "Analysis of ride comfort on the stairs climbing wheelchair," *Advances in Human Aspects of Transportation: Part II*, vol. 16, no. II, 2021, doi: 10.54941/ahfe100674.

[26] P. Chawaphan, D. Maneetham, P. N. Crisnapati, and R. J. Liou, "A novel stair-climbing robot controlled using the internet of things," In *2023 11th International Conference on Cyber and IT Service Management (CITSM)*, 2023, doi: 10.1109/CITSM60085.2023.10455194.

[27] S. S. Waydande, H. Deshmukh, K. Gopalghare, S. Patil, and J. Shirke, "Design & development of stair climbing robot prototype," *Journal of Emerging Technologies and Innovative Research (JETIR)*, vol. 11, no. 7, pp. 53–58, Jul. 2024.

[28] L. Bruzzone, M. Baggetta, S. E. Nodehi, P. Bilancia, and P. Fanghella, "Functional design of a hybrid leg-wheel-track ground mobile robot," *Machines*, vol. 9, no. 1, pp. 1–11, 2021, doi: 10.3390/machines9010010.

[29] B. Sharma, B. M. Pillai, K. Borvorntanajanya, and J. Suthakorn, "Modeling and design of a stair climbing wheelchair with pose estimation and adjustment," *Journal of Intelligent and Robotic Systems: Theory and Applications*, vol. 106, no. 3, 2022, doi: 10.1007/s10846-022-01765-3.

[30] A. A. Jorge, L. A. M. Riascos, and P. E. Miyagi, "Modelling and controlling of a hybrid motorized wheelchair on flat and inclined surfaces," in *2019 6th International Conference on Control, Decision and Information Technologies, CoDIT 2019*, 2019, pp. 750–755, doi: 10.1109/CoDIT.2019.8820679.

[31] W. Yu, W. Dazhi, and Z. Yufeng, "Intelligent wheelchair obstacle avoidance design based on fuzzy PID control," *Journal of*

Shanghai University of Engineering Science, vol. 38, no. 3, pp. 250–256, 2024, doi: 10.12299/jsues.23-0216.
[32] T. Kara and A. H. Mary, "Adaptive PD-SMC for nonlinear robotic manipulator tracking control," *Studies in Informatics and Control*, vol. 26, no. 1, pp. 49–58, 2017, doi: 10.24846/v26i1y201706.
[33] H. V. Thu, T. T. Thi, T. N. Thi, B. N. Hai, and D. V. Van, "Application of an adaptive dynamic sliding surface controller with traction tracking for a Mecanum Wheel mobile robot," *Journal of Robotics and Control (JRC)*, vol. 6, no. 2, pp. 1051–1060, Apr. 2025, doi: 10.18196/jrc.v6i2.23693.

BIOGRAPHIES OF AUTHORS

Duong Tan Dat was born in 1992, Vinh Long City, Vietnam. He is currently a lecturer and working at Vinh Long University of Technology Education. He received his engineering degree in 2017 from Saigon University of Technology, and his master's degree in 2019 from Ho Chi Minh City University of Technical Education. Major in training in mechatronic engineering technology, automation systems. Research fields: robots, smart devices, automation systems. He can be contacted at email: datdt@vlute.edu.vn.

Le Hong Ky was born in 1963 in Vietnam. He received his engineering degree in 1987 with a major in machine design and his master's degree in 1996 from Ho Chi Minh City University of Technical Education with a major in machine manufacturing. He studied in Korea in 1995, in Canada in 2006, in Singapore in 2019 with majors in CAD/CAM-CNC, competency-based training (CBT), multimedia and e-learning, education and technical training. He is currently a lecturer and former vice principal of Vinh Long University of Technology Education. Research fields include machine manufacturing, special machining methods, optimization of machining processes such as grinding, EDM machining, and optimal gearbox design. He can be contacted at email: kylh@vlute.edu.vn.

Tran Duc Thuan was born in 1956 in Bac Ninh, Vietnam. He received his degree in remote control engineering from Moscow Power Engineering University in 1980, and his Ph.D. in technical cybernetics and information theory in 1983 from Moscow Power Engineering University. He was appointed associate professor in 1984 at the Institute of Science and Technology under the Ministry of National Defense of Vietnam. He was Head of the Missile Control Research Department (1997-2008), Head of the Doctoral Training Department (2008-2014), Specialist (2014-2019), retired (from 2019 to present) and is currently a full-time teacher at Vinh Long University of Technology Education (from 2019 to present). Research fields: Automation, control of moving objects with modern control methods (adaptive control, optimal control, sliding control, invariant control). He can be contacted at email: thuandauto@yahoo.com.